Open access • Journal Article • DOI:10.1063/1.4747719

Mechanical properties of graphynes under tension: A molecular dynamics study

Yingyan Zhang, Qing-Xiang Pei, Chen Wang

Published on: 22 Aug 2012 - Applied Physics Letters (American Institute of Physics)

Topics: Graphyne

Mechanical properties of graphynes under tension: A molecular dynamics study

Y. Y. Zhang' , Q. X. Pei' , and C. M. Wang

Citation: Appl. Phys. Lett. **101**, 081909 (2012); doi: 10.1063/1.4747719
View online: http://dx.doi.org/10.1063/1.4747719
View Table of Contents: http://aip.scitation.org/toc/apl/101/8
Published by the American Institute of Physics

Mechanical properties of graphynes under tension: A molecular dynamics study

Y. Y. Zhang,[1,a)] Q. X. Pei,[2,b)] and C. M. Wang[3]
[1]*School of Computing, Engineering and Mathematics, University of Western Sydney, South Penrith, NSW 2751, Australia*
[2]*Institute of High Performance Computing, A*STAR, Singapore 138632, Singapore*
[3]*Engineering Science Programme and Department of Civil and Environmental Engineering, National University of Singapore, Kent Ridge, Singapore 119260*

(Received 6 May 2012; accepted 8 August 2012; published online 22 August 2012)

Graphyne is the allotrope of graphene. In this letter, four different graphynes (α, β, γ, and 6,6,12-graphenes) are investigated by molecular dynamics simulations to explore their mechanical properties and failure mechanisms. It is found that the presence of the acetylenic linkages in graphynes leads to a significant reduction in fracture stress and Young's modulus with the degree of reduction being proportional to the percentage of the linkages. This deterioration in mechanical properties stems from the low atom density in graphynes and weak single bonds in the acetylenic linkages where the facture is initiated. © *2012 American Institute of Physics*. [http://dx.doi.org/10.1063/1.4747719]

Graphene has stirred a considerable interest around the world since it was discovered in 2004.[1] Extensive research studies have been conducted to explore its unique properties and potential applications.[1–4] Along with the graphene surge, attempts have been made to find its carbon allotropes, e.g., graphynes or graphdiynes. Like graphene, graphynes are also one-atom-thick sheet of carbon atoms but with different atomic bonds. In addition to the sp^2 carbon bonds, graphynes contain *sp* hybridized bonds. The presence of the *sp* carbon atoms destroys the regular hexagonal crystal lattice of the graphene. This allows for the formation of various types of graphynes with different geometries.[5–10] Figure 1 shows four different types of graphynes, namely α-, β-, γ-, and the 6,6,12-graphynes.[11] These graphynes differ from each other with regard to the percentage of the acetylenic linkage ($-C \equiv C-$) in their structures. In addition to studying their electronic properties,[5–11] efforts have also been devoted to study their mechanical properties. Recently, Cranford and Buehler[12] performed an atomistic study on the γ-graphyne (see Fig. 1(d)) and found that its fracture stress and strain show strong anisotropy. Using first-principle calculations, Kang *et al.*[13] found that the γ-graphyne is much softer than graphene. Yang and Xu[14] explored the mechanical properties of γ-graphyne and its graphyne groups. However, the mechanical properties of other types of graphynes, such as the α-, β-, and 6,6,12-graphynes considered in Ref. 11, have not been investigated. This motivated us to investigate the mechanical properties of all the four different types of graphynes using molecular dynamics (MD) simulations. We will not only characterize the Young's modulus, fracture stress, and strain but also examine the failure mechanisms of graphynes.

Graphynes may be regarded as formed by replacing certain percentages of carbon-carbon sp^2 bonds in graphene by the acetylenic linkages. The α-graphyne in Fig. 1(b) has a similar atomic geometry as that of graphene in Fig. 1(a), but all the carbon-carbon sp^2 bonds have been replaced by the acetylenic linkages. The percentages of the acetylenic linkages are 66.67%, 33.33%, and 41.67% for the β-, γ-, and 6,6,12-graphynes, respectively. It is expected that the introduction of different densities of the linkages in graphynes should make their mechanical properties interestingly different from those of graphene.

In the MD simulations, all the models are approximately square with a side length of approximately 20 nm. Using graphene as the reference, zigzag and armchair edges are oriented along the *x* and *y* directions, respectively. The software package LAMMPS (Ref. 15) is used for the MD simulations. The interaction between the carbon atoms is described by the adaptive intermolecular reactive empirical bond order (AIREBO) potential,[16] which has been widely used to investigate the mechanical and thermal properties of carbon-based nanomaterials.[17–24] Uniaxial tensile loading is applied either along the *x* or *y* direction at a strain rate of 0.0005 ps^{-1} with a time step of 0.5 fs. The environmental temperature is maintained at 300 K by using the Nosé-Hoover thermostat.[25,26] Periodic boundary conditions are applied along the *x* and *y* directions to eliminate the edge effects. Prior to loading, the initial configuration is optimized by using the conjugate gradient method and then the system is relaxed in NPT (i.e., constant atom number, pressure, and temperature) ensemble for 100 ps. In order to overcome spuriously high tensile force when the carbon-carbon bond length is greater than 1.7 Å, the onset of the covalent interaction cutoff distance is increased to 2.0 Å[19–23] in the AIREBO potential.

The simulated stress-strain curves for graphynes and graphene subjected to uniaxial tension in *x* and *y* directions are shown in Figs. 2(a) and 2(b), respectively. In the determination of the stress, the thickness of the structures is assumed to be 0.335 nm. Herein, the fracture stress is defined as the peak stress and the corresponding strain is the fracture strain. From Fig. 2, it is seen that graphene displays a linear stress-strain relationship when the tensional strain is small (say <0.05); thereafter the stress increases nonlinearly with the strain until fracture occurs. However, all the graphynes

a)Electronic mail: yingyan.zhang@uws.edu.au.
b)Electronic mail: peiqx@ihpc.a-star.edu.sg.

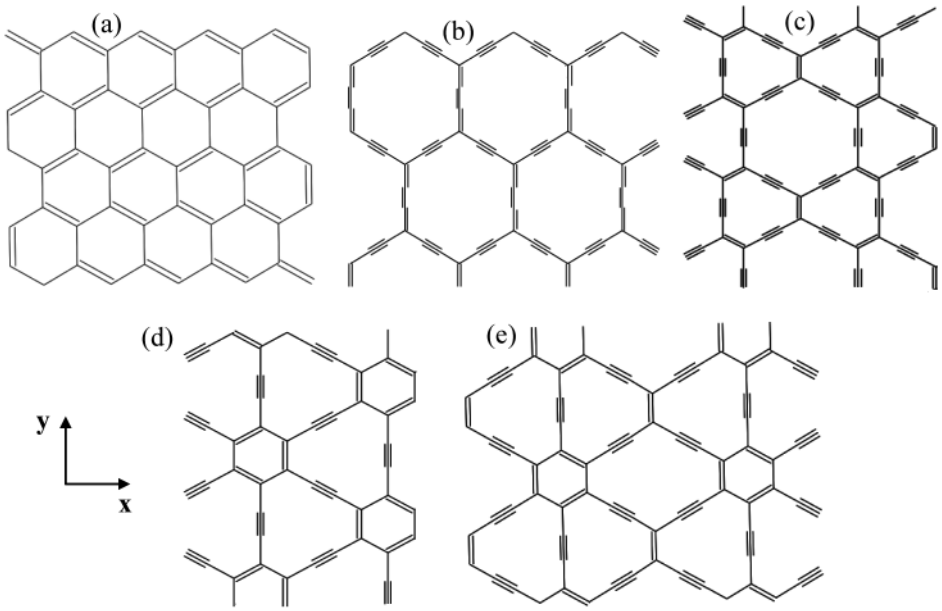

FIG. 1. Bonding structures of graphene and graphynes. (a) Graphene; (b) α-graphyne; (c) β-graphyne; (d) γ-graphyne; (e) 6,6,12-graphyne.

display approximately linear stress-strain relationships before fracture, indicating that graphynes are more brittle than graphene. Fig. 2 clearly shows that graphene has a higher fracture stress in both x and y directions than the graphynes. Our simulated fracture stresses of graphene are 125.18 and 103.56 GPa in the x (zigzag) and y (armchair) directions, respectively, which are somewhat close to 137 and 105 GPa obtained by Pei *et al.*[22] and to 107 and 90 GPa obtained by Zhu *et al.*[19] These results agree well with the experimental value of 123.5 GPa.[3] The fracture strains of graphene in zigzag and armchair directions are 0.191 and 0.134, respectively, which are in very good agreement with 0.2 and 0.13 given by Zhu *et al.*[19] From Table I, it can be seen that the fracture stresses of graphynes range from 32.48 to 63.17 GPa, which are about 1/3 to 1/2 of those of graphene. It is also observed from Table I that the fracture stress and strain of graphene and graphynes in the zigzag (x) direction are higher than those in the armchair (y) direction. The direction-dependent properties can be explained as follows. Fig. 1 shows that some bonds in graphene and graphynes are parallel to the y (armchair) direction, while no bonds in those structures are parallel to the x (zigzag) direction. When the tensile loading is applied in the y direction, those bonds parallel to the y direction will undergo stress and deformation directly in the bond-length direction, which causes the bond elongation and breaking. In contrast, when the same tensile loading is applied in the x direction, the loading is not in the bond-length direction, thereby it has not so strong effect on the bond elongation in the bond-length direction. This difference in the bond orientation results in anisotropic fracture properties.

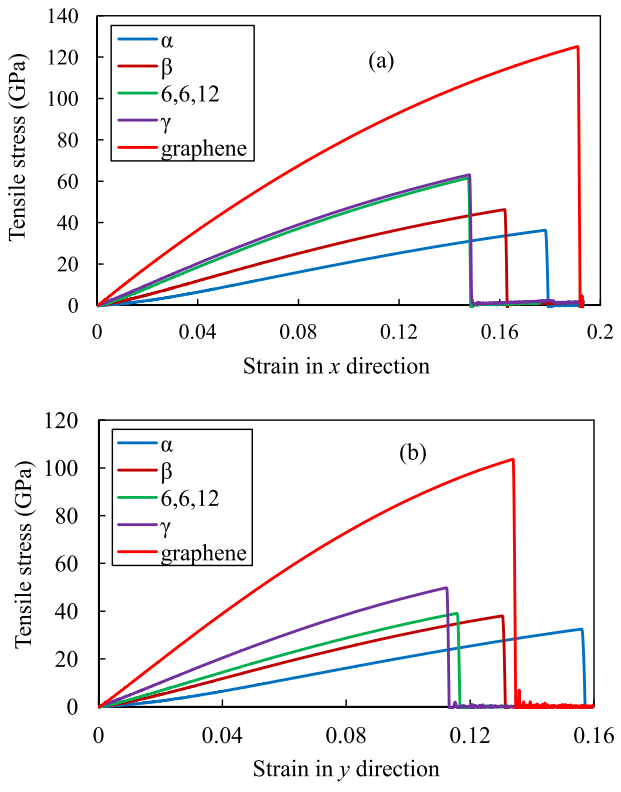

FIG. 2. Stress-strain curves of graphynes and graphene under tensile loading (a) in the x (zigzag) and (b) y (armchair) direction.

It can be seen from Fig. 2 and Table I that graphene possesses the highest fracture stress in the x directions, followed by γ-, 6,6,12-, β-, and α-graphynes. The same trend is also observed in the y direction. It is interesting to find from Table I that the fracture stresses of the four different graphynes depend heavily on the percentage of the acetylenic linkages in their structures. The fracture stress of graphynes decreases with increasing linkages. This may be attributed to the different atom densities of the structures caused by the different percentages of the linkages. With the increase of the linkages in graphynes from γ-graphyne (33.33%) to α-graphyne (100%), the atom density drops from 29.61 to 18.92 atoms/nm^2. The sparser carbon atoms in the structures lead to less bond connections and consequently a smaller fracture stress.

From Table I, it is also found that the 6,6,12-graphyne possesses the highest degree of directional anisotropy with 36.61% difference in fracture stress. This is because all the graphynes and graphene have hexagonal symmetry except 6,6,12-graphyne.[11] Malko *et al.*[11] reported that 6,6,12-graphyne possesses the directional anisotropy in electronic property. This directional anisotropy in mechanical and electronic

TABLE I. Fracture stresses, strains, and Young's moduli of graphynes and graphene.

Model	Percentage of acetylenic linkage	Atom density (atoms/nm^2)	Stress (GPa)		Difference in stresses (%)	Strain		Difference in strains (%)	Young's modulus (TPa)	
			x	y		x	y		x	y
α	100	18.92	36.36	32.48	10.69	0.178	0.156	12.37	0.12	0.119
β	66.67	23.13	46.26	38.06	17.72	0.162	0.130	19.54	0.261	0.26
6,6,12	41.67	28.02	61.62	39.06	36.61	0.147	0.116	21.54	0.445	0.35
γ	33.33	29.61	63.17	49.78	21.20	0.148	0.112	24.09	0.505	0.508
Graphene	0	39.95	125.2	103.6	17.27	0.191	0.134	29.93	0.995	0.996

properties could make 6,6,12-graphyne more versatile in potential applications.

In contrast to the fracture stress, the fracture strains of graphynes display an opposite trend with respect to the percentage of the acetylenic linkages as shown in Fig. 2 and Table I. The fracture strains increase with increasing percentage of the linkages. The presence of the linkages in graphyne leads to a reduction in fracture stress, but it makes the graphyne flexible and thereby it enhances the fracture strain accordingly. As the linkages make the graphyne less rigid, they have a strong effect on the Young's modulus.

The Young's moduli of graphynes and graphene can be obtained from the stress-strain data in Fig. 2 by using the Hooke's law $\sigma = E\epsilon$ at small strain level (≤ 0.02). This is to assure that the structures are in the linear deformation region and Hooke's law is valid for the determination of the Young's modulus. The Young's moduli of graphene and graphynes are listed in Table I. Similar to the trend of fracture stresses, graphene possesses the highest Young's modulus of 0.995 TPa and 0.996 TPa in the x and y directions, respectively, which agree well with the experimental value of 1 TPa.[3] For graphynes, the presence of the acetylenic linkages leads to a significant reduction in Young's modulus. A higher percentage of the linkages in graphyne results in a lower Young's modulus due to lower atom densities of the structures. The Young's modulus of graphynes ranges from 0.12 to 0.505 TPa, which is much lower than that of graphene. It can be seen that the 6,6,12-graphyne demonstrates a strong anisotropy in Young's modulus. For the other graphynes and graphene, their Young's moduli in the x and y directions are rather close, indicating little anisotropy in Young's modulus.

In order to explore the fracture mechanism of graphynes, we now study the stress distributions and the fracture processes of graphynes. Herein, the fractured morphologies of 6,6,12-graphyne are demonstrated in Fig. 3 for the illustrative purpose. When the graphynes are subjected to the x-axial tension, the acetylenic linkages in the inclined direction show a higher stress than the linkages in the vertical (y) direction (see the stress distribution before fracture in Fig. 3(a)), meaning that the inclined linkages undergo a larger tensile deformation. Since the single bonds are weaker than the triple ones, the bond breaking will occur at the single bonds in the inclined linkages upon further deformation. This can be confirmed from the corresponding fractured morphology in Fig. 3(b). The zoomed view in Fig. 3(b) clearly displays that the bond breaking occurs in the single bonds (highlighted in blue) of the inclined acetylenic linkages at the fracture strain. Therefore, the single bonds in the linkages undermine the fracture properties. Under tension, the single bonds in the linkages break first and become the origin of the crack as shown in Fig. 3. Then the crack spreads to all the directions on further loading, causing the graphyne to rupture finally.

For the graphynes under the y-axial tension, the vertical acetylenic linkages in graphynes show higher stress as shown in Fig. 3(d). Since the single bonds are weaker than the triple ones, bond breaking is expected to occur at the single bonds in the vertical linkages upon further tension deformation, which is

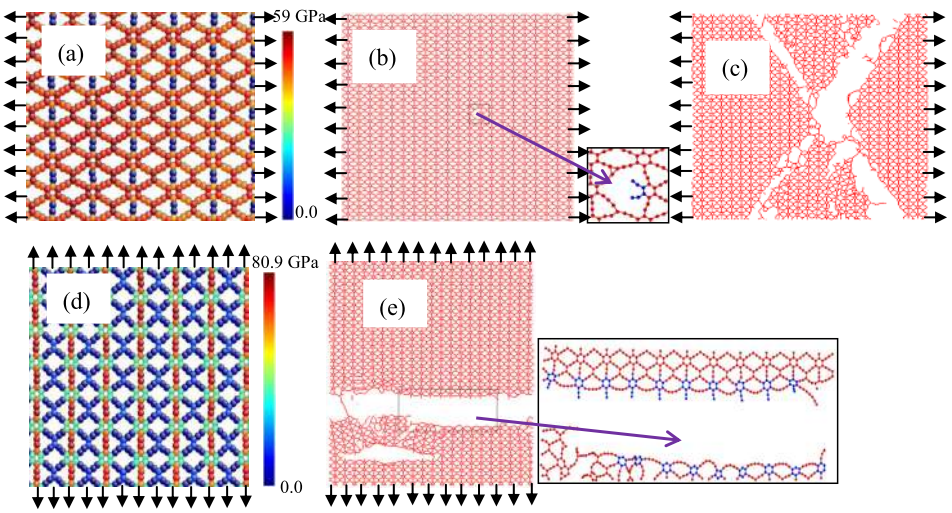

FIG. 3. The 6,6,12-graphyne under tensile loading. (a) Stress distribution at strain of 0.1 under tensile loading in the x direction; (b)-(c) morphologies at strains of 0.145 and 0.147 before and after fracture for the x-direction loading; (d) stress distribution at strain of 0.1 under tensile loading in the y direction; (e) fractured morphology at fracture strain of 0.116 for the y-direction loading.

supported by the zoomed fractured part in Fig. 3(e) and matches very well with the high stress distributions in Fig. 3(d).

In summary, we have studied the mechanical properties and failure mechanisms of graphynes under uniaxial tension by using MD simulations. It is found that the presence of the acetylenic linkages in graphynes has a pronounced effect on the mechanical properties. The fracture stress and Young's modulus decrease with increasing percentage of the linkages. But it is the reverse trend for the fracture strain. The induced effects by the linkages stem from the low atom density with the associated less bond connections and the weak single bonds in the linkages. Among the four different graphynes, 6,6,12-graphyne displays very obvious directional anisotropy in the mechanical properties. Along with its highly anisotropic electrical conductivity,[11] 6,6,12-graphyne may be more versatile in potential applications. The present work offer insights for better understanding the mechanical properties and failure mechanism of graphynes.

Y. Y. Zhang is grateful for the financial support provided by Research lectureship [20731–81465] and IRIS [P00020285] in the University of Western Sydney, Australia. This work was also supported by the NCI National Facility at the ANU.

[1]K. S. Novoselov, A. K. Geim, S. V. Morozov, D. Jiang, Y. Zhang, S. V. Dubonos, I. V. Grigorieva, and A. A. Firsov, Science **306**, 666 (2004).
[2]K. Geim and K. Novoselov, Nature Mater. **6**, 183–191 (2007).
[3]C. Lee, X. Wei, J. W. Kysar, and J. Hone, Science **321**, 385–388 (2008).
[4]A. Balandin, Nature Mater. **10**, 569–581 (2011).
[5]R. H. Baughman, H. Eckhardt, and M. Kertesz, J. Chem. Phys. **87**, 6687–6699 (1987).
[6]V. R. Coluci, S. F. Braga, S. B. Legoas, D. S. Galvao, and R. H. Baughman, Nanotechnology **15**, S142–149 (2004).
[7]E. H. L. Falcao and F. Wudl, J. Chem. Technol. Biotechnol. **82**, 524–531(2007).
[8]A. Hirsch, Nature Mater. **9**, 868–871 (2010).
[9]G. X. Li, Y. L. Li, H. B. Liu, Y. B. Guo, Y. J. Li, and D. B. Zhu, Chem. Commun. **46**, 3256–3258 (2010).
[10]A. N. Enyashin and A. L. Ivanovskii, Phys. Stat. Sol. B **248**, 1879–1883 (2011).
[11]D. Malko, C. Neiss, F. Vines, and A. Gorling, Phys. Rev. Lett. **108**, 086804 (2012).
[12]S. W. Cranford and M. J. Buehler, Carbon **49**, 4111–4121 (2011).
[13]J. Kang, J. Li, F. Wu, S. S. Li, and J. B. Xia, J. Phys. Chem. C **115**, 20466–2047 (2011).
[14]Y. Yang and X. Xu, Comput. Mater. Sci. **61**, 83–88 (2012).
[15]S. J. Plimpton, J. Comput. Phys. **117**, 1–19 (1995).
[16]S. J. Stuart, A. B. Tutein, and J. A. Harrison, J. Chem. Phys. **112**, 6472–6486 (2000).
[17]C. Tang, W. L. Guo, and C. F. Chen, Phys. Rev. Lett. **100**, 175501 (2008).
[18]B. W. Jeong, J. K. Lim, and S. B. Sinnott, Appl. Phys. Lett. **90**, 023102 (2007).
[19]H. Zhao, K. Min, and N. R. Aluru, Nano Lett. **9**, 3012–3015 (2009).
[20]R. Grantab, V. B. Shenoy, and R. S. Ruoff, Science **330**, 946–948 (2010).
[21]Y. Y. Zhang, C. M. Wang, Y. Cheng, and Y. Xiang, Carbon **49**, 4511–4517 (2011).
[22]Q. X. Pei, Y. W. Zhang, and V. B. Shenoy, Nanotechnology **21**,115709 (2010).
[23]Q. X. Pei, Y. W. Zhang, and V. B. Shenoy, Carbon **48**, 898–904 (2010).
[24]A. Bagri, S. P. Kim, R. S. Ruoff, and V. B. Shenoy, Nano Lett. **11**, 3917–3921(2011).
[25]S. Nose, J. Chem. Phys. **81**, 511–519 (1984).
[26]W. G. Hoover, Phys. Rev. A **31**, 1695–1697 (1985).